

Compressive Loading-Unloading Behavior of Nuclear Graphite Grades of Different Forming Method and Raw Cokes

Se-Hwan Chi*, Seong-Deok Hong, Yong-Wan Kim
Nuclear Hydrogen Development and Demonstration Project, KAERI,
Dae Duk Science Town, Yuseong, Daejeon 305-353 Rep. of Korea
*Corresponding author: shchi@kaeri.re.kr

1. Introduction

Nuclear graphite is used for core structural components and neutron moderators in high-temperature gas-cooled reactors. As graphite is a brittle material fail at relatively low strains (e.g., ~0.5% in tension and ~2% in compression), cracking of these components can occur throughout the life of the reactor under the influence of thermal and mechanical stresses [1-3]. While a lot of studies have been performed on the fracture of graphite, most studies have been concerned on crack initiation and propagation [3], with little concerns on the damage processes that lead to the very first stage of crack initiation.

In this study, the graphite damage processes before the main crack formation were investigated based on the microstructure change during load relaxation. For this, 4-1/3 notched flexure strength test specimens made of nuclear graphite grades IG-110, NBG-18 and PCEA of different forming methods (isotropic molding, vibrational molding and extrusion, respectively) and ingredients (coke, binder) were subjected to 10 cyclic compressive loading-unloading, and the changes in the microstructure of notch-tip areas were examined by X-ray tomography.

2. Experimental

2.1 Materials and specimen

Table 1 summarizes the characteristics of the grades selected for this study. For NBG and PCEA grades, the forming (molding) direction was considered (NBG-18-a, NBG-18-c, PCEA-a, PCEA-c), where **a** and **c** refer to the notch direction machined to the “molding direction” and “perpendicular to the molding direction,” respectively. 4-1/3 flexure loading specimens were machined at a size of 16 mm (width) x 18 mm (thickness) x 64 mm (length) with a notch (width: 0.1 mm, length: 7.2 mm, angle: $<30 \pm 2^\circ$). Ten specimens were prepared for each grade.

2.2 Flexure loading and relaxation load measurement.

To investigate the grade dependent loading-unloading and load relaxation behaviors under cyclic compressive loading-unloading, specimens were subjected to 10 cyclic loading-unloadings under compression at room temperature (compression displacement = 0.13 mm,

cross head velocity: 0.5 mm/min).

Table 1 characteristics of the grades.

| Grade | Manufacturer | Form. Meth. | Co. Type | G.S (av. μm) | Den. (g/cm ³) |
|--------|--------------|-------------|----------|--------------------------|---------------------------|
| NBG-18 | SGL | Vibr. | Pitch | 300 | 1.85 |
| PCEA | Graf. | Extr. | Pet. | 360 | 1.87 |
| IG-110 | Toyo Tanso | Iso-Mo | Pet. | 20 | 1.77 |

The 0.13 mm compression displacement employed in the present study correspond to about 0.81 (IG-110, NBG) and 0.87 (PCEA) fracture displacements, and to about 0.65 (NBG-18-c), 0.68 (NBG-18-a, PCEA), 0.75 (PCEA-a), and 0.97 (IG-110) fracture loads, respectively. During cyclic loading-unloading, the load-displacement curves were obtained.

2.3 X-ray tomography

To investigate the changes in the microstructure, and thus the cause of load relaxation at the notch tip area, specimens for X-ray tomography at a size of 3 x 3 x 15 mm³ were machined from the notch area after cyclic compressive loading-unloading using a diamond saw. **Figure 1** shows the schematics of specimen preparation from the notch area and the set-up for X-ray tomography (Model: WALISCHMILLER RAY SCAN 250).

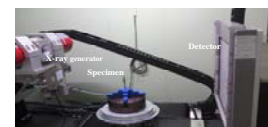
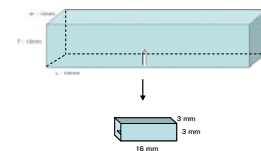


Fig. 1 the schematics of specimen preparation from the notch area and the set-up for X-ray tomography.

The conditions for X-ray tomography are: a voxel size of 9.7 μm at 90 KeV and 110 μA for IG-110, and a voxel

size of 11.02 μm at 100 KeV and 130 μA for NBG and PCEA. The scanned data were processed using VX3D software (3D Industrial and Imaging. www.3Dii.kr) for pore analysis and 3-D visualization of an internal microstructure change (crack formation).

3. Results and Discussion

3.1 Loading-unloading behavior and relaxation load

Figure 2 shows an example of the load-displacement curves of the NBG-18-**a** and **c** during the 10 cyclic compressive loading-unloadings, and **Table 2** compares the relaxation load during the cyclic loading.

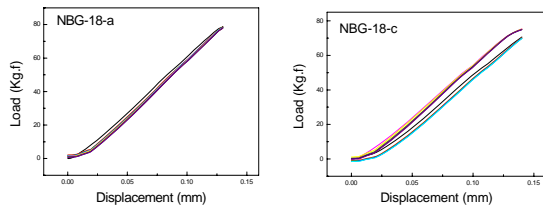


Figure 2 Cyclic loading-unloading curves of NBG-18-a and c.

Table 2 Comparison of the relaxation load after 10 loading-unloading cycles (compressive loading displacement: 0.13 mm).

| Grade | Initial load before unloading (Kg) | Relaxation load (Kg) during the first 10 cycles | Relaxation load (%) |
|------------|------------------------------------|---|---------------------|
| IG-110 | 59.2 | 0.7 | 1.18 |
| NBG-18 (a) | 75.3 | 0.3 | 0.40 |
| NBG-18 (c) | 78.8 | 0.9 | 1.14 |
| PCEA (a) | 75.8 | 0.2 | 0.26 |
| PCEA (c) | 70.4 | 0.9 | 1.28 |

As seen in **Figure 2**, all the grades showed grade specific loading-unloading behaviors reflecting different microstructures and damage accommodation characteristics.

NBG-18 and **PCEA** showed an apparent anisotropy in loading-unloading behavior. Both grades in **c** direction showed an unstable and large hysteresis and relaxation load compared with the **a** direction. It is of note that the relaxation loads in **c** are about 3 and 5 times larger than the **a** direction in NBG and PCEA, respectively, and is worth noting that the relaxation load appears larger in PCEA with a larger average grain size (360 μm) than NBG-18 with a smaller one (300 μm). NBG-18 and PCEA show a similar loading-unloading behaviors in the **a** direction.

3.2 Microstructure change by X-Ray tomography

Figure 3 shows an examples of 3 dimensional microstructures obtained from X-ray tomography before (as-received) and after 10 cyclic compressive loading-unloadings.

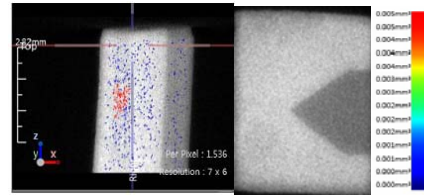


Fig. 3 An example of X-ray tomography for IG-110 specimen (3 x 3 x 16 mm³) after cyclic loading.

Results of X-ray tomography showed no crack formation below and around the notch. The number of pores decreased 29 - 40 %, and the total volume of pores increased 47 - 150 %. The PCEA showed the least decrease in the number of pores (29%) and the least increase in the total pore volume (~ 47%). The NBG of the vibrational molding shows the largest decrease in the number of pores (40%) and the largest increase in the total pore volume (150%). Large differences in the change of the pore structures owing to the differences in the forming methods of the grades and raw ingredients are noted. The weak particle-binder interfaces are thought to be a major source of pores, where fine cracks will be formed during the grain re-orientation under the cyclic compressive loading-unloading. The changes in the pore structures suggest the clustering and coalescence of the pores and a new pore formation, possibly by grain (coke)-binder interface separation or grain reorientation along the **c** direction.

4. Conclusion

Without the crack formation, all the grades showed a grade dependent load relaxation (0.26 ~ 1.28%) and a decrease in the number of pores and an increase in the total pore volume. These pore structure changes were attributed to the clustering/coalescence of pores (decrease in the number of pores) and the evolution of new pores from the grain (coke)-binder interfaces along the **c** direction during cyclic loading - unloading (increase in the total volume of pores).

REFERENCES

- [1] T. H. Becker, T. J. Marrow, R. B. Tait, JNM 414 (2011) 32-43
- [2] Generation IV Reactors Integrated Materials Technology Program Plan : Focus on Very High Temperature Reactor Materials, ORNL/TM-2008/129 (2008)
- [3] A. P. G. Rose and M. O. Tucker, JNM 110 (1982) 186-195